

*mathematical model of vehicle, multibody system simulation,  
dynamic simulation*

*Maria TOMASIKOVA<sup>\*</sup>, Frantisek BRUMERČÍK<sup>\*\*</sup>,  
Aleksander NIEOCZYM<sup>\*\*\*</sup>*

## DESIGN AND DYNAMICS MODELING FOR ELECTRIC VEHICLE

### Abstract

*This paper describes software for vehicle simulation and mathematical models that describe the motion of the vehicle. A dynamic simulation model of vehicle was developed using Matlab/Simulink and SimDriveline toolbox. The model has a configurable structure that is suitable to simulation with multiple levels. The powertrain system model developed using Simulink and SimDriveline could also be used as a generic, modular and flexible vehicle modeling platform to support the integration of powertrain design and control system optimization.*

### 1. INTRODUCTION

The dynamic behavior of vehicles can be analysed in several different ways. One way may be a simple spring mass system, through a three-degree of freedom (DoF) model, to a large degree of complexity using a multibody system simulation package such as MSC ADAMS or Modelica. Vehicle models are often simulated with advanced controller designs provided as software in the loop (SIL) with controller design software such as Simulink, or with physical hardware in the loop (HIL). The subject of modeling in Simulink and SimDriveline

---

<sup>\*</sup> University of Zilina, Faculty of Mechanical Engineering, Univerzitná 1, 010 26 Žilina, Slovakia, e-mail: tomasikovam@fstroj.uniza.sk

<sup>\*\*</sup> University of Zilina, Faculty of Mechanical Engineering, Univerzitná 1, 010 26 Žilina, Slovakia, e-mail: frantisek.brumercik@fstroj.uniza.sk

<sup>\*\*\*</sup> Lublin University of Technology, Faculty of Mechanical Engineering, Nadbystrzycka 36, 20-618 Lublin, Poland, e-mail: a.nieoczym@pollub.pl

was presented in (Tomasikova, Nieoczym & Brumerick, 2015; Tomasikova, Brumerick & Nieoczym, 2015). The issues of structural modeling and electric vehicle dynamics using Simulink are described in several publications. In (Cheng, Dong & Dong, 2013) powertrain model of a series-parallel, multiple-regime plug-in hybrid electric vehicle (SPMR-PHEV) was introduced. Simulation and control system was developed using rule-based load-leveling energy management strategy (EMS) under the MATLAB/Simulink and SimDriveline environment. The powertrain system model developed using Simulink and SimDriveline could also be used as a generic, modular and flexible vehicle modeling platform to support the integration of powertrain design and control system optimization.

A dynamic simulation model of electric vehicle (EV) was developed using Matlab/Simulink and SimPowerSystem/SimDriveline toolbox. The EV model has a configurable structure that is suitable to simulation with multiple fidelity levels. This advantage will combine simulation models associated with deployment and test for different controllers to a single platform. It has multiple running rates and different solvers for subsystems in order to speed up simulation. The electrical system model is capable to simulate power electronics behavior both on average and switching level. An automated mechanical transmission (AMT) model and its controller were developed for heavy duty application, such as a city bus (Zhou , Shen & Liu, 2014).

Mousavi, Saman, Pakniyat & Boulet (2014) focuses on the modeling, simulation and control of a two-speed transmission for electric vehicles which has seamless gear shifting specification. The transmission incorporates two-stage planetary gear sets and two braking mechanisms to control the gear shifting. The dynamic model is developed by using the kinematic equations of the planetary gear trains and the Euler-Lagrange equations to derive the equations of motion. The mathematical model is validated by using the SimDriveLine library of MATLAB/Simulink.

During construction work related to vehicle modeling, there are problems with formalizing the physical processes occurring in the vehicle. A test vehicle was created to validate the mathematical model. It 's experimental research and demonstration vehicle – Research Concept Vehicle (RCV) (Wallmark & Nybacka, 2014). The vehicle is intended as a platform to implement, validate, and demonstrate research results from different research projects carried out at KTH. In (Fang et al., 2013; Pawlus, Hovland & Choux, 2015) characterized the driveline modelling techniques for development of new control algorithms. This paper presents the analysis of the current driveline modelling methods through comparison simulations in Matlab. A driveline model including the tyre dynamics is developed and its effectiveness has been demonstrated by simulations.

## 2. VEHICLE MODEL

Vehicle model is created in Matlab-SimDriveline. The blocks represent basic parts of vehicle like engine, gear, differential, tires. The model contains elementary information about vehicle geometry – dimensions and center of gravity position. These information about vehicle are sufficient for mathematical description of vehicle.

Key features:

- Common gear configuration models, including planetary, differential, and worm gears with meshing and viscous losses.
- Clutch models.
- Vehicle component models, including engine, torque converter, and vehicle dynamics models.
- Models of translational elements.
- Ideal and non-ideal model variants, enabling adjustment of model fidelity.

### 2.1. Engine block

The engine model is specified by an engine power demand function  $g(\omega)$ . The function provides the maximum power available for a given engine speed  $\omega$ . The block parameters (maximum power, speed at maximum power and maximum speed) normalize this function to physical maximum torque and speed values.

The engine power is nonzero when the speed is limited to the operating range

$$\omega_{min} \leq \omega \leq \omega_{max} \quad (1)$$

The absolute maximum engine power  $Pmax$  defines  $\omega_0$  such that  $Pmax = g(\omega_0)$ . Define  $w \equiv \omega/\omega_0$  and  $g(\omega) \equiv Pmax \cdot p(w)$ .

Then  $p(1) = 1$  and  $dp(1)/dw = 0$ .

The torque function is:

$$\tau = (Pmax/\omega_0) \cdot [p(w)/w] \quad (2)$$

Generic engine uses a third-order polynomial form:

$$p(w) = p_1 \cdot w + p_2 \cdot w^2 - p_3 \quad (3)$$

In typical engines, the  $p_i$  are positive. This polynomial has three zeros, one at  $w = 0$ , and a conjugate pair. One of the pair is positive and physical; the other is negative and unphysical:

$$\omega_{\pm} = 1/2 \left( -p_2 \pm \sqrt{p_2^2 + 4 p_1 p_2} \right) \quad (4)$$

For the engine power polynomial, there are restrictions on the polynomial coefficients  $p_i$ , to achieve a valid power-speed curve. These restrictions are detailed below. If you use tabulated power or torque data, corresponding restrictions on  $P(\omega)$  remain.

Set:

- $w = \omega/\omega_0$  and  $p = P(\omega)/P_0$ ,
- $w_{min} = \omega_{min}/\omega_0$  and  $w_{max} = \omega_{max}/\omega_0$ .

Then engine speed is restricted to a positive range above the minimum speed and below the maximum speed:

$$0 \leq w_{min} \leq w \leq w_{max} \quad (5)$$

The engine power at minimum speed must be nonnegative:  $p(w_{min}) \geq 0$ . If you use the polynomial form, this condition is a restriction on the  $p_i$ :

$$p(w_{min}) = p_1 \cdot w_{min} + p_2 \cdot w_{min}^2 - p_3 \cdot w_{min}^3 \geq 0 \quad (6)$$

The engine power at maximum speed must be nonnegative:

$$p(w_{max}) \geq 0.$$

If you use the polynomial form, this condition is a restriction on:

$$w_{max}: w_{max} \leq w_+.$$

For the default parametrization, Generic Engine provides two choices of engine, each with different engine power demand parameters (Table 1).

**Tab. 1. Engine power demand parameters**

Power demand coefficient	Engine type	
	Spark ignition	Diesel
$p_1$	1	0.6256
$p_2$	1	1.6948
$p_3$	1	1.3474

## 2.2. Gear block

The Simple Gear block represents a gearbox that constrains the two connected driveline axes, base (B) and follower (F), to co rotate with a fixed ratio that you specify. You can choose whether the follower axis rotates in the same or opposite direction as the base axis. If they rotate in the same direction,  $\omega_F$  and  $\omega_B$  have the same sign. If they rotate in opposite directions,  $\omega_F$  and  $\omega_B$  have opposite signs.

Simple Gear imposes one kinematic constraint on the two connected axes:

$$r_F \omega_F = r_B \omega_B \quad (7)$$

The follower-base gear ratio  $u_{FB} = z_F/z_B$ , where  $z$  is the number of teeth on each gear. The two degrees of freedom reduce to one independent degree of freedom. The torque transfer is:

$$u_{FB} T_B + T_F - T_{loss} = 0 \quad (8)$$

In the ideal case moment of losses in the system  $T_{loss} = 0$ .

In a nonideal gear pair, the angular velocity, gear radii, and gear teeth constraints are unchanged. But the transferred torque and power are reduced by:

- Coulomb friction between teeth surfaces on gears, characterized by efficiency  $\eta$ ,
- Viscous coupling parametrized by viscous friction coefficients  $\mu$ :
- 

$$T_{loss} = T_{Coul} \cdot \tanh\left(\frac{4\omega_{out}}{\omega_{th}}\right) + \mu\omega_{out}, \quad (9)$$

$$T_{Coul} = |T_F| \cdot (1 - \eta). \quad (10)$$

where:  $T_{loss}$  – moment of losses in the system,

$T_{Coul}$  – moment on coupling.

Conditions (Jeong & Lee, 2000):

- Constant Efficiency: in the constant efficiency case,  $\eta$  is constant, independent of load or power transferred.
- Load-Dependent Efficiency: in the load-dependent efficiency case,  $\eta$  depends on the load or power transferred across the gears.

For either power flow:

$$T_{Coul} = u_{FB} T_{idle} + k T_F, \quad (11)$$

Factor  $k$  is a proportionality constant. Coefficient  $\eta$  is related to  $T_{Coul}$  in the standard, preceding form but becomes dependent on load:

$$\eta = T_F/[u_{FB}T_{idle} + (k + 1)T_F]. \quad (12)$$

This block has limitations, also:

- Gear inertia is assumed negligible,
- Gears are treated as rigid components.

Differential gear block represents a gear mechanism that allows the driven shafts to spin at different speeds. Differentials are common in automobiles, where they enable the various wheels to spin at different speeds while cornering. Ports S, D1, and D2 represent the driving and driven shafts of the differential. Any of the shafts can drive the remaining two.

The block models the differential mechanism as a structural component based on Simple Gear and Sun-Planet Bevel Simscape™ Driveline™ blocks. Fig. 1 shows the block diagram of this structural component.

Differential imposes one kinematic constraint on the three connected axes:

$$\omega_D = \pm(1/2)u_D(\omega_{S1} + \omega_{S2}), \quad (13)$$

with the upper (+) or lower (-) sign valid for the differential crown to the right or left, respectively, of the center-line. The three degrees of freedom reduce to two independent degrees of freedom. The gear pairs are (1,2) = (S,S) and (C,D). C is the carrier.

The *sum* of the lateral motions is the transformed longitudinal motion. The difference of side motions  $\omega_{S1} - \omega_{S2}$  is independent of the longitudinal motion. The general motion of the lateral shafts is a superposition of these two independent degrees of freedom, which have this physical significance. One degree of freedom (longitudinal) is equivalent to the two lateral shafts rotating at the same angular velocity ( $\omega_{S1} = \omega_{S2}$ ) and at a fixed ratio with respect to the longitudinal shaft.

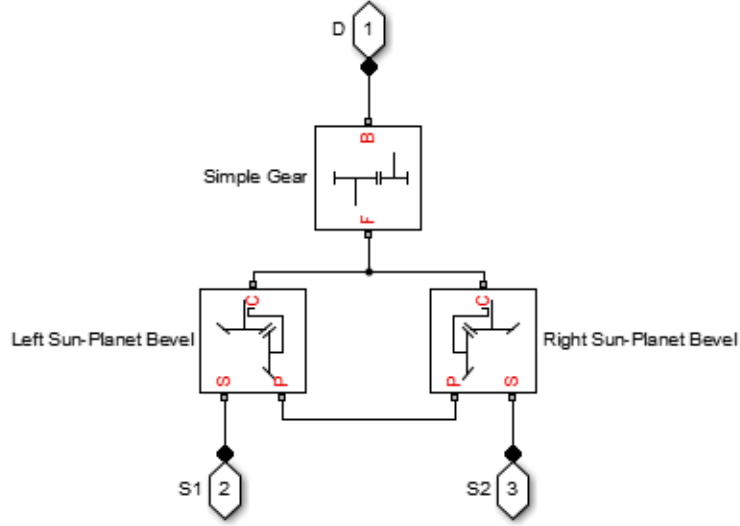


Fig. 1. The structural component of differential block

The other degree of freedom (differential) is equivalent to keeping the longitudinal shaft locked ( $\omega_D = 0$ ) while the lateral shafts rotate with respect to each other in opposite directions ( $\omega_{S1} = -\omega_{S2}$ ).

The torques along the lateral axes,  $T_{S1}$  and  $T_{S2}$ , are constrained to the longitudinal torque  $T_D$  in such a way that the power flows into and out of the gear, less any power loss  $N_{loss}$ , sum to zero:

$$\omega_{S1}T_{S1} + \omega_{S2}T_{S2} + \omega_D T_D - P_{loss} = 0 \quad (12)$$

When the kinematic and power constraints are combined, the ideal case yields:

$$u_D T_D = 2(\omega_{S1}T_{S1} + \omega_{S2}T_{S2}) / (\omega_{S1} + \omega_{S2}) \quad (13)$$

### 2.3. Tire block

The Tire Block models the tire as a rigid wheel-tire combination in contact with the road and subject to slip. When torque is applied to the wheel axle, the tire pushes on the ground (while subject to contact friction) and transfers the resulting reaction as a force back on the wheel. If you include the optional tire compliance, the tire also flexibly deforms under load. Table 2 defines the tire model variables. Forces and Characteristic Function: a tire model provides a steady-state tire characteristic function  $F_x = f(\kappa, F_z)$ , the longitudinal force  $F_x$  on the tire, based on vertical load  $F_z$  and wheel slip  $\kappa$

**Tab. 2. The tire model variables**

<b>Parameter</b>	<b>Description</b>
$r_w$	Wheel radius
$v_x$	Wheel hub longitudinal velocity
$u$	Tire longitudinal deformation
$\Omega$	Wheel angular velocity
$\Omega'$	Contact point angular velocity = $\Omega$ if $u = 0$
$r_{w\Omega'}$	Tire tread longitudinal velocity
$v_{sx} = r_{w\Omega} - v_x$	Wheel slip velocity
$v'_{sx} = r_{w\Omega'} - v_x$	Contact slip velocity = $v_{sx}$ if $u = 0$
$\kappa = v_{sx}/ v_x $	Wheel slip
$\kappa' = v'_{sx}/ v_x $	Contact slip = $\kappa$ if $u = 0$
$v_{th}$	Wheel hub threshold velocity
$F_z$	Vertical load on tire
$F_x$	Longitudinal force exerted on the tire at the contact point.
$C_{F_x} = (\partial F_x / \partial u)_0$	Tire longitudinal stiffness under deformation
$b_{F_x} = (\partial F_x / \partial \dot{u})_0$	Tire longitudinal damping under deformation
$I_w$	Wheel-tire inertia
$T_{drive}$	Torque applied by the axle to the wheel

Each tire in The Pacejka “Magic formula” (Pacejka, 2005) is characterized by 10–20 coefficients for each important force that it can produce at the contact patch, typically lateral and longitudinal force, and self-aligning torque, as a best fit between experimental data and the model. These coefficients are then used to generate equations showing how much force is generated for a given vertical load on the tire, camber angle and slip angle. A problem with Pacejka's model is that when implemented into computer code, it doesn't work for low speeds (from around the pit-entry speed), because a velocity term in the denominator makes the formula diverge (Kucera, Lukac, Jurak & Brumerick, 2009).

The Magic Formula is a specific form for the tire characteristic function, characterized by four dimensionless coefficients (B, C, D, E), or stiffness, shape, peak, and curvature:

$$\begin{aligned}
 F_x &= f(\kappa, F_z) = \\
 &= F_z \cdot D \cdot \sin(C \cdot \arctan[\{ B\kappa - E \cdot [ B\kappa - \arctan(B\kappa) ] \}])
 \end{aligned} \tag{14}$$

A more general Magic Formula uses dimensionless coefficients that are functions of the tire load. A more complex set of parameters  $p, I$  entered in the dialog box, specifies these functions:

$$F_{x0} = D_x \cdot \sin(C_x \cdot \arctan[\{ B_{x\kappa} - E_x [ B_{x\kappa} - \arctan(B_{x\kappa}) ] \}]) + S_{Vx} \quad (15)$$

where:  $df_z = (F_z - F_{z0})/F_z$ ,

$$\kappa_x = \kappa + S_{Hx},$$

$$C_x = p_{Cx1},$$

$$D_x = \mu_x \cdot F_z,$$

$$\mu_x = p_{Dx1} + p_{Dx2} \cdot df_z,$$

$$E_x = (p_{Ex1} + p_{Ex2} \cdot df_z + p_{Ex3} \cdot df_z^2)[1 - p_{Ex4} \cdot \text{sgn}(\kappa_x)],$$

$$K_{x\kappa} = F_z \cdot (p_{Kx1} + p_{Kx2} \cdot df_z) \cdot \exp(p_{Kx3} \cdot df_z),$$

$$B_x = K_{x\kappa} / (C_x D_x + \varepsilon_x),$$

$$S_{Hx} = p_{Hx1} + p_{Hx2} \cdot df_z,$$

$$S_{Vx} = F_z \cdot (p_{Vx1} + p_{Vx2} \cdot df_z).$$

$S_{Hx}$  and  $S_{Vx}$  represent offsets to the slip and longitudinal force in the force-slip function, or horizontal and vertical offsets if the function is plotted as a curve.  $\mu_x$  is the longitudinal load-dependent friction coefficient.  $\varepsilon_x$  is a small number inserted to prevent division by zero as  $F_z$  approaches zero.

The block uses a representative set of Magic Formula coefficients. The block scales the coefficients to yield the peak longitudinal force  $F_{x0}$  at the corresponding slip  $\kappa_0$  that you specify, for rated vertical load  $F_{z0}$ .

Numerical values are based on empirical tire data. These values are typical sets of constant Magic Formula coefficients for common road conditions.

**Tab. 3. Formula coefficient**

Surface	B	C	D	E
Dry tarmac	10	1.9	1	0.97
Wet tarmac	12	2.3	0.82	1
Snow	5	2	0.3	1
Ice	4	2	0.1	1

## 2.4. Vehicle body block

This block models a vehicle with two axles in longitudinal motion. The axles can have different wheel counts. The vehicle wheels are assumed identical in size. The vehicle axles are parallel and form a plane. The longitudinal  $x$  direction lies in this plane and perpendicular to the axles. The vehicle motion is

determined by the net effect of all the forces and torques acting on it. The longitudinal tire forces push the vehicle forward or backward. The weight  $mg$  of the vehicle acts through its centre of gravity (CG). Figure 2 and Table 4 define the vehicle motion model variables.

This are the motion equations:

$$m \dot{V}_x = F_x - F_d - mg \sin \beta \quad (16)$$

$$F_x = n(F_{xf} + F_{xr}) \quad (17)$$

$$F_d = \frac{1}{2} C_d \rho A (V_x - V_w)^2 \quad (18)$$

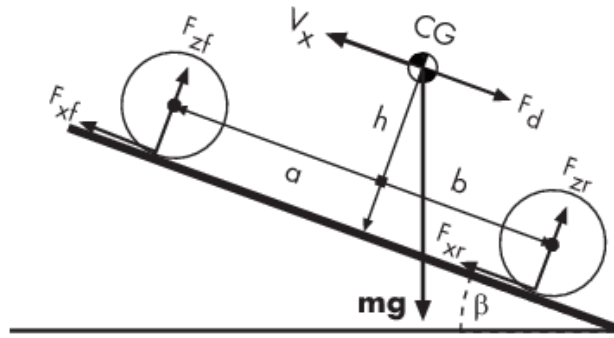


Fig. 2. Scheme of the vehicle model

Zero normal acceleration and zero pitch torque determine the normal force on each front and rear wheel:

$$F_{zf} = \frac{-h (F_d + mg \sin \beta + m \dot{V}_x) + b mg \cos \beta}{n(a+b)} \quad (19)$$

$$F_{zr} = \frac{+h (F_d + mg \sin \beta + m \dot{V}_x) + a mg \cos \beta}{n(a+b)} \quad (20)$$

**Tab. 4. The vehicle motion model variables**

<b>Parameter</b>	<b>Description</b>
$\beta$	Incline angle
$h$	Height of vehicle CG above the ground
$a, b$	Distance of front and rear axles, respectively, from the normal projection point of vehicle CG onto the common axle plane
$v_x$	Longitudinal vehicle velocity
$v_w$	Headwind speed
$n$	Number of wheels on each axle
$F_{xf}, F_{xr}$	Longitudinal forces on each wheel at the front and rear ground contact points, respectively
$F_{zf}, F_{zr}$	Normal load forces on the each wheel at the front and rear ground contact points, respectively
$A$	Effective frontal vehicle cross-sectional area
$C_d$	Aerodynamic drag coefficient
$\rho$	Mass density of air $\rho = 1.2 \text{ kg/m}^3$
$F_d$	Aerodynamic drag force

The Vehicle Body block lets you model only longitudinal dynamics, parallel to the ground and oriented along the direction of motion. The vehicle is assumed to be in pitch and normal equilibrium. The block does not model pitch or vertical movement. As such, the equations assume that the wheels never lose contact. This constraint can result in negative normal forces.

Vehicle model in SimDriveline is simplified 4 wheels car (Figure 3). We can measure and explore some dynamic properties of vehicle like vehicle velocity, normal forces on tire, wheel rpm. The model is limited. We can simulate only driving in direct direction, not turning. The Tire (Magic Formula) block assumes longitudinal motion only and includes no camber, turning, or lateral motion.



### 3. CONCLUSIONS

The methodology for designing the propulsion and driving system using the Simulink program has been presented. The analyzed driving system was divided into functional components: engine, clutch, gearbox and powertrain with rubber wheels. For each component, key features and model limitations were identified. The basic formulas and the mathematical relationships used in modeling have been demonstrated. Mathematical formulas are written in a parametric manner using coefficients. The coefficients values are given for the calculation of the propulsion engine, the driving wheels and the dynamic effects on the vehicle. The equations described above allow for quick analysis of the output when changing certain coefficients. A model vehicle built from Simulink blocks. This model takes into account the kinematic dependence on vehicle units and enables analysis of dynamic vehicle characteristics. Limitation of the described model is the analysis of its motion on the straight line.

### REFERENTS

- Fang, Ch., Cao, Z., Ektesabi, M., Kapoor, A., & Sayem, A. (2013). Driveline modelling analysis for active driveability control. In *Systems, Process & Control (ICSPC), 2013 IEEE Conference*. Kuala Lumpur, Malaysia: IEEE. doi:10.1109/SPC.2013.6735117
- Jeong, H., & Lee, K. (2000). Friction coefficient, torque estimation, smooth shift control law for an automatic power transmission. *KSME International Journal*, 14(5), 508–517. doi:10.1007/BF03185653
- Mousavi, M., Saman, R., Pakniyat, A., & Boulet, B. (2014). Dynamic modeling and controller design for a seamless two-speed transmission for electric vehicles. *Control Applications (CCA), 2014 IEEE Conference*. Juan Les Antibes, France: IEEE. doi:10.1109/CCA.2014.6981411
- Kucera, L., Lukac, M., Jurak, L., & Brumerick, F. (2009). Hydromechanical automatic transmission. *Communications*, 11(2), 33–35.
- Pacejka, H. (2005). *Tyre and vehicle dynamics*. Elsevier.
- Pawlus, W., Hovland, G., & Choux, M. (2015). Drivetrain design optimization for electrically actuated systems via mixed integer programming. In *Industrial Electronics Society, IECON 2015 – 41st Annual Conference of the IEEE*. Yokohama, Japan: IEEE. doi:10.1109/IECON.2015.7392307
- Cheng, R., Dong, J., & Dong, Z. (2013). Modelling and simulation of a multiple-regime plug-in hybrid electric vehicle. In *ASME 2013 International Design Engineering Technical Conferences and Computers and Information in Engineering Conference (I)*, pp. V001T01A009). Portland, Oregon, USA. doi:10.1115/DETC2013-13619
- Tomasikova, M., Nieozym, A., & Brumerick, F. (2015). Vehicle drivetrain modelling. In *Transcom Proceedings 2015, 11-th European Conference of Young Researches and Scientists* (pp.265-268). Zilina, Slovak Republic.
- Tomasikova, M., Brumerick, F., & Nieozym, A. (2015). *Vehicle simulation model creation*. LOGI, Scientific Journal on Transport and Logistics, 6(1), 130–136.
- Wallmark, O., & Nybacka M. (2014). Design and implementation of an experimental research and concept demonstration vehicle. In *Vehicle Power and Propulsion Conference (VPPC), 2014 IEEE*. Coimbra, Portugal: IEEE. doi:10.1109/VPPC.2014.7007042
- Zhou, J., Shen, X., & Liu, D. (2014). Modeling and simulation for electric vehicle powertrain controls. In *Transportation Electrification Asia-Pacific (ITEC Asia-Pacific), 2014 IEEE Conference and Expo*. Beijing, China: IEEE. doi: 10.1109/ITEC-AP.2014.6940824